Available online at www.sciencedirect.com
ScienceDirect
Sensors and Actuators A 141 (2008) 640–648
SENSORS AND ACTUATORS A PHYSICAL
www.elsevier.com/locate/sna

Design, fabrication, and experimental characterization of a flap valve IPMC micropump with a flexibly supported diaphragm

Thanh Tung Nguyen [a,c], Nam Seo Goo [b,c,*,1], Vinh Khanh Nguyen [c], Youngtai Yoo [d], Seungbae Park [e]

[a] *Department of Aerospace Engineering, Konkuk University, Gwangjin-gu, Seoul 143-701, Republic of Korea*
[b] *Smart Microsystem Research Laboratory, Department of Advanced Technology Fusion, Konkuk University, Gwangjin-gu, Seoul 143-701, Republic of Korea*
[c] *Artificial Muscle Research Center and Smart Robot Center, Konkuk University, Gwangjin-gu, Seoul 143-701, Republic of Korea*
[d] *Department of Materials Chemistry and Engineering, Konkuk University, Gwangjin-gu, Seoul 143-701, Republic of Korea*
[e] *Department of Mechanical Engineering, State University of New York at Binghamton, NY 13902, USA*

Received 9 October 2006; received in revised form 28 September 2007; accepted 30 September 2007
Available online 13 October 2007

Abstract

This paper presents the design, fabrication and experimental characterization of a flap valve ionic polymer–metal composite (IPMC) micropump, the diaphragm of which is supported by a flexible material. A multilayered IPMC based on a Nafion/layered silicate and Nafion/silica nanocomposites was fabricated and used as an actuator for the micropump. To make best use of a flexible IPMC diaphragm, we introduced a concept of flexible support and implemented the concept by supporting an IPMC actuator with a compliant polydimethylsiloxane (PDMS) structure at its perimeter. We then fabricated an IPMC micropump with the IPMC diaphragm and flap valves made from the PDMS material. Experiments and finite element analyses were performed to justify the concept of flexible support and to characterize the multilayered IPMC diaphragm and the IPMC micropump. A maximum flow rate of 760 μl/min and a maximum backpressure of 1.5 kPa were recorded at an applied voltage of 3 V and a driving frequency of 3 Hz, even though the performance lasted for a few minutes. The proposed micropump is attractive due to its low operational voltage, lack of leakage problems, simple design, and ease of manufacturing.

Keywords: Microfluidics; IPMC; Micropump; Flap valve; PDMS; Flexible support concept

1. Introduction

A typical microelectromechanical system, the micropump is an essential element in microfluidic systems or lab-on-a-chip technology. For the last three decades, numerous micropumps have been developed and they can be categorized by their valve types as either a one-way check valve or a valveless micropump. Furthermore, micropumps can be grouped according to their driving mechanisms, which may be based on such actuations as piezoelectric, shape memory alloy, electromagnetic, pneumatic, thermopneumatic, or electrostatic actuations [1,2]. Of these driving mechanisms, the piezoelectric actuations are the most popular for micropump applications because they normally have a short response time and a high output force, though their high operational voltages and small volume stroke are considered disadvantages [3,4]. The other actuation mechanisms seem to be less popular in micropump applications due to disadvantages such as the long response time in shape memory alloys [5], the large size of the electromagnetic and pneumatic actuations [6], the high temperatures and high power consumption in thermopneumatic actuations [7], and the low output force and small stroke in electrostatic actuations [8].

Recently, ionic polymer–metal composites (IPMCs) have attracted considerable attention due to their large deformation at low applied voltages, relatively short response times and

* Corresponding author at: Department of Advanced Technology Fusion, Konkuk University, Gwangjin-gu, Seoul 143-701, Republic of Korea.
Tel.: +82 2 450 4133; fax: +82 2 444 7091.
E-mail address: nsgoo@konkuk.ac.kr (N.S. Goo).
[1] Temporarily visiting Professor of State University of New York at Binghamton, USA (February 2007 to January 2008).

0924-4247/$ – see front matter © 2007 Elsevier B.V. All rights reserved.
doi:10.1016/j.sna.2007.09.017

biocompatibility characteristics. Even though IPMCs can operate well in dry environments when fabricated as self-contained encapsulated actuators [9], they can perform well in a humid environment. Thus, IPMCs are considered to be promising candidates for micropump applications, particularly for use in a humid environment. However, a survey of the literature reveals a dearth of IPMC micropump research. Guo et al. reported an IPMC micropump with active valves made from IPMC and a doubled chamber: their micropump reached a maximum flow rate of 37.8 μl/min [10]. Pak et al. presented a valveless IPMC micropump with a maximum flow rate of 9.97 μl/min; the durability and sealing of the IPMC diaphragm were reported as drawbacks [11]. Although these authors [10,11] provided only scant details about their micropump structures, the micropumps had a common diaphragm support structure: namely, the IPMC actuator was firmly fixed at its perimeter. The firmly fixed condition of flexible IPMC diaphragms might constrain the movement of the IPMC diaphragm, causing the micropumps to produce relatively low flow rates. In a review paper, Shahinpoor and Kim described an IPMC micropump with ball valves as one of the industrial applications of IPMCs [12]. Unfortunately, the details of this micropump were not found in the literature. Recently, Lee et al. reported a design and flow rate estimation of a valveless IPMC micropump, the flow rate of which was estimated analytically to be as high as 8.2 μl/s [13,14].

We present a flap valve IPMC micropump with a flexibly supported diaphragm. An effective diaphragm-supporting design appears to be better than a conventional fixed support design, especially in terms of producing a large actuation displacement of the IPMC diaphragm and enhancing the pumping performance. Hence, we supported the IPMC diaphragm with a flexible structure fabricated from PDMS material. We also designed a flap valve because an IPMC valveless micropump barely overcomes the backpressure that arises as a result of the low operational frequency of IPMC actuators [15]. The flap valve was made of PDMS material, which has advantages such as good sealing properties, transparent characteristics, desirable mechanical properties, and ease of processing with micromolding techniques [16,17]. We used finite element analysis to investigate the actuation performance as well as the natural frequencies of the IPMC diaphragm and the PDMS flap valve. After fabricating the proposed micropump with PDMS molding and a conventional milling technique, we tested the performance of pumping action. The experimental results and test observations confirm that the proposed IPMC micropump can produce a substantial flow rate and pumping pressure, and that the good sealing property of PDMS material in the new support design can solve the sealing problem.

2. Design, fabrication, and modeling of an IPMC diaphragm

2.1. Concept of flexible support

Fig. 1(a) and (b) shows the typical support methods of an IPMC diaphragm. Generally, the simply support method

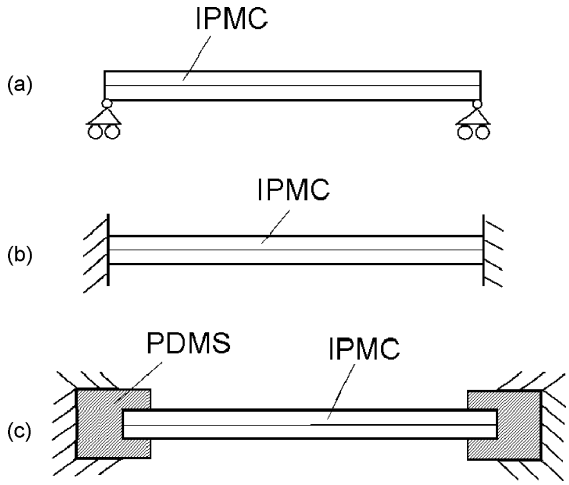

Fig. 1. Support methods of IPMC diaphragms: (a) an IPMC diaphragm simply supported at its perimeter; (b) an IPMC diaphragm fixed at its perimeter; (c) an IPMC diaphragm supported at its perimeter by a flexible PDMS structure.

(Fig. 1(a)) can produce larger actuation displacement than the fixed support method (Fig. 1(b)) under the same driving voltage. In the prior works [10,11], the IPMC diaphragms were fixed at their perimeter, as shown in Fig. 1(b) and this type of support is likely to constrain the movement of a relatively flexible IPMC actuator. With these facts in mind, another support method of IPMC diaphragm is attempted to make best of IPMC diaphragm. Even though the simply support method can produce larger actuation displacement, it is not easy to implement due to the sealing problem. Thus, we propose to use PDMS material, as shown in Fig. 1(c), to develop a flexible support method. Given the low level of stiffness and the good sealing property of PDMS material, our design does not constrain the movement of an IPMC actuator.

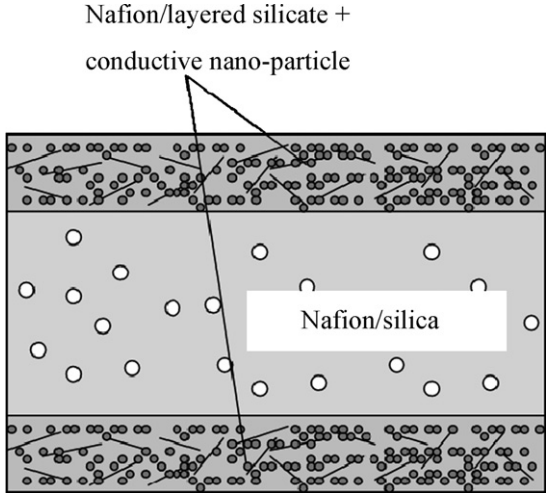

Fig. 2. Configuration of the multilayered IPMC; the Nafion/modified silica layer is sandwiched between two thinner layers containing Nafion, layered silicate, and conductive material particles (Ag nanopowder).

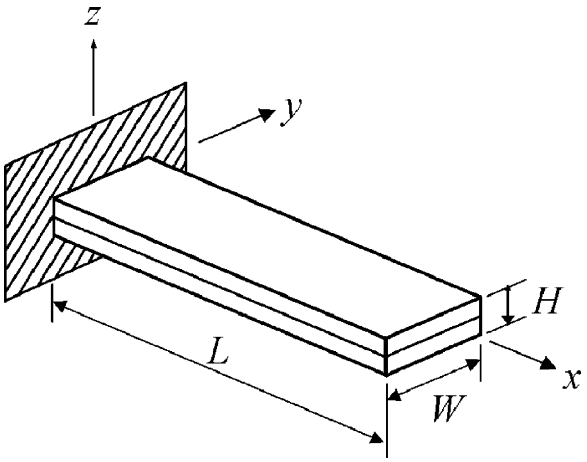

Fig. 3. Equivalent bimorph beam model for IPMC actuators.

2.2. A multilayered IPMC and equivalent bimorph beam modeling

To make the IPMC diaphragm, as shown in Fig. 2, we used a multilayered IPMC developed by the third and fourth authors of the present paper [18,19]. The multilayered IPMC, which was fabricated with a consecutive recasting method, consists of a main Nafion/modified silica layer sandwiched between two thinner layers containing Nafion, layered silicate, and conductive material particles (Ag nanopowder). The blocking force of the IPMC was improved significantly without any sacrifice in its displacement. More details of the IPMC can be found elsewhere [18,19]. We fabricated the IPMC so that it had a thickness of approximately 0.6 mm, which was sufficient to produce enough actuation force for pumping purposes.

To assess the actuation performance of IPMC diaphragms with different support methods, we used finite element analysis (FEA) together with the equivalent bimorph beam model for IPMC actuators proposed by Lee et al. [13,14]. In the model, as shown in Fig. 3, an IPMC actuator is assumed to be composed of two identical virtual layers. The application of an electric field across an IPMC actuator is equivalent to a contraction of one layer and an expansion of the other.

The calculations for the equivalent electromechanical coupling coefficient, d_{31}, and the equivalent elastic modulus, E, which are based on the measured tip displacement, s, the measured blocking force, F_{bl}, the applied voltage, V, and the geometry sizes of the equivalent beam, are expressed as follows [13,14]:

$$d_{31} = \frac{2sH^2}{3L^2V} \tag{1}$$

and

$$E = \frac{8LF_{bl}}{3WHd_{31}V}. \tag{2}$$

To determine the necessary coefficients in the equivalent bimorph beam model, we measured the blocking force and the displacement. Several IPMC strips with dimensions of 20 mm × 5 mm × 0.6 mm were cut from the fabricated IPMCs. For the blocking force measurement, we clamped the IPMC strip at one end and placed the other end in contact with a load cell (Dacell, CB1-G150). Next, when the electric field was applied through the clamped end, the tip force acting on the load cell was recorded with a data acquisition system. We then measured the displacement by using a non-contact laser sensor (KEYENCE LK-G80). Table 1 shows the experimental results of a cantilevered IPMC strip at the applied ac voltages of 1 V, 2 V and 3 V with a driving frequency of 1 Hz, as well as the necessary coefficients for the equivalent bimorph beam model. Note that we used half the value of the up-and-down tip displacement listed in Table 1 to calculate the equivalent electromechanical coupling coefficient, d_{31}.

2.3. Fabrication of an IPMC diaphragm

Fig. 4(a) describes the fabrication process of the IPMC diaphragm. First, we created a 50 μm-thick SU-8 mold on a silicon wafer by using a standard photolithography process. Next, we used a PDMS molding technique to create a thin PDMS membrane, with a thickness of 100 μm, on the SU-8 mold. To attach the IPMC actuator to the PDMS membrane, we used a layer of uncured PDMS. After curing the PDMS layer with the attached IPMC actuator at room temperature for 24 h, we covered the IPMC actuator with a thin layer of PDMS and then thermally cured the coated IPMC actuator. Finally, we used a cutting device to remove parts of the lower and upper PDMS layers that covered the IPMC actuator, thereby enabling the IPMC actuator to be in direct contact with the water inside the pump chamber. The direct contact of IPMC actuator with the water helps increase the durability of the IPMC actuator. Fig. 4(b) shows a photograph of the fabricated IPMC diaphragm. We found that the PDMS structure of the IPMC diaphragm provides a complete seal between the IPMC actuator and the pump chamber. Note also that we used a 1:10 (curing agent: PDMS) mixing ratio for the PDMS molding.

Table 1
Characteristics and material properties of the fabricated IPMC actuator

Applied voltage (V ac)	Size (mm^3)	Blocking force (gf)	Tip displacement (mm)	d_{31} (10^{-7} m/V)	Young's modulus (GPa)
1	20 × 5 × 0.6	0.9	1.6	4.8	0.35
2	20 × 5 × 0.6	2.9	3.4	5.1	0.51
3	20 × 5 × 0.6	5.8	5.6	5.6	0.61

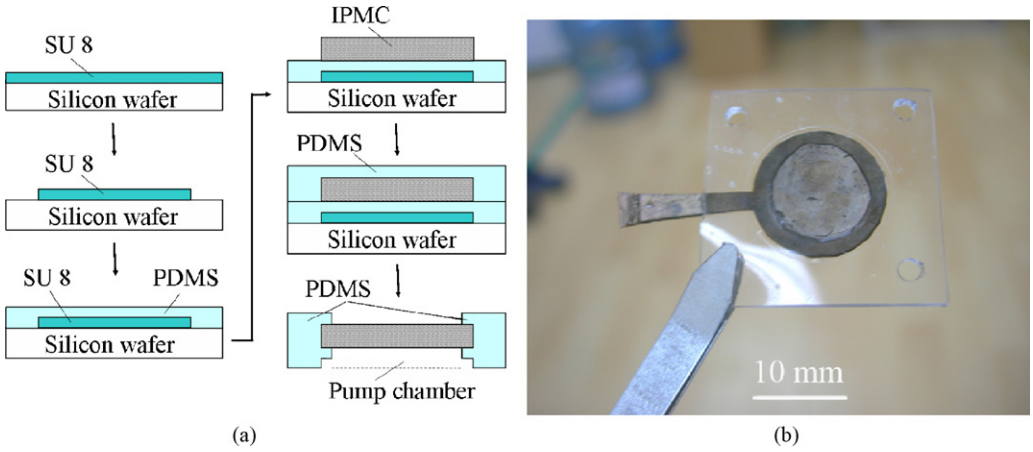

Fig. 4. A multilayered IPMC diaphragm: (a) the fabrication process of the IPMC diaphragm with photolithography and PDMS molding techniques and (b) a photograph of the fabricated IPMC diaphragm with a 14 mm diameter and a 0.6 mm-thick IPMC actuator.

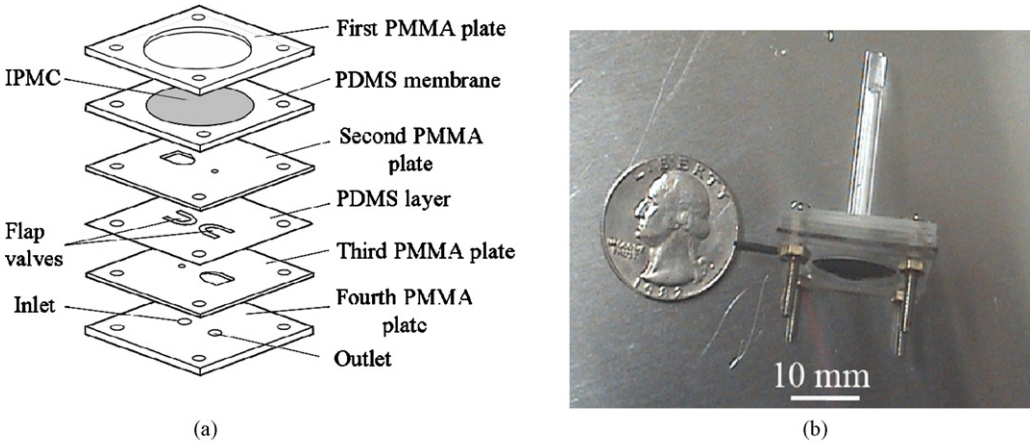

Fig. 5. The IPMC micropump with a flexible support design: (a) structure of the micropump with six stacked layers and (b) photograph of the fabricated micropump.

3. Design and fabrication of a flap valve IPMC micropump

We designed a flap valve micropump with a multilayered IPMC diaphragm, as described in Section 2. Fig. 5 illustrates the structure and shows a photograph of the fabricated IPMC micropump. The micropump is composed of six layers of the same size. The first layer is a polymethyl methacrylate (PMMA) plate, which has an opening of 14 mm in diameter at the center; the second layer is the IPMC diaphragm described in Section 2; the third layer is made from PMMA and has two holes for a valve seal and outlet. The pump chamber is defined by the space between the second layer and the third layer. The fourth layer has two PDMS flap valves, which are described later. The fifth layer is identical to the third layer. In the third and fifth layer, the size of the valve orifices is 1 mm in diameter. The sixth layer, fabricated from PMMA, has an inlet hole and an outlet hole, both of which are connected to the corresponding inlet and outlet piles. The PMMA parts were fabricated by means of conventional computer numerical control (CNC) machining. Each

Table 2
Summary of analyses and experiments performed during the development of the IPMC micropump

	Title	Purpose	Result
Analysis	Static analysis of the IPMC diaphragm	To justify the equivalent bimorph beam model and to calculate a blocking force–displacement diagram for three support methods	Figs. 9 and 10
	Vibration analysis of the IPMC diaphragm and a flap valve	To determine the natural frequencies	Table 3
Experiment	Actuation performance of the IPMC diaphragm	To justify the equivalent bimorph beam model	Figs. 8 and 9
	Pumping performance of the IPMC micropump	To asses the pumping performance of the IPMC micropump	Fig. 11
	Durability test of the IPMC micropump	To evaluate the durability of the IPMC micropump	Fig. 12

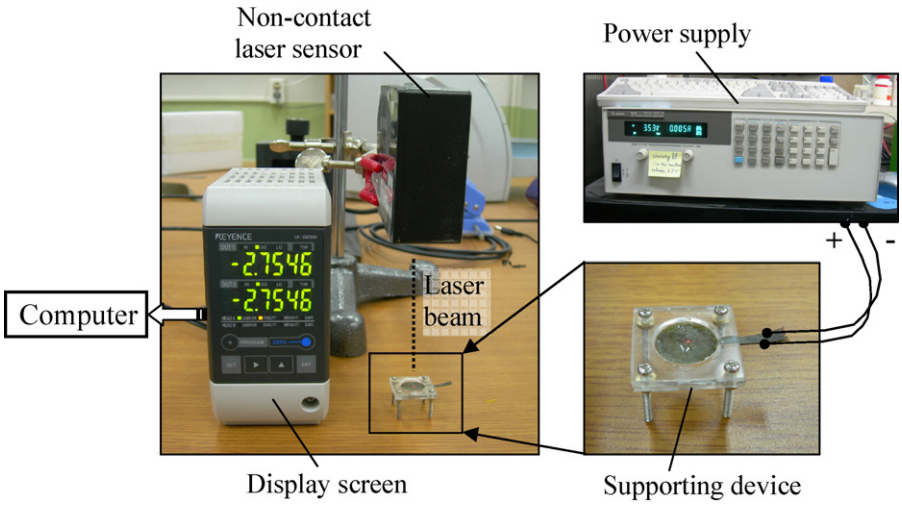

Fig. 6. Apparatus for the actuation test of the IPMC diaphragm. The system consists of a digital power supply, a non-contact laser sensor (KEYENCY LK-G80), a computer, and a supporting device.

layer has four screw holes in the corners so that the layers can be stacked and held fast with four screws. Finally, as shown in Fig. 5(b), glass pipes were connected to the inlet and outlet holes to complete the micropump. The overall size of the micropump is 20 mm × 20 mm × 5 mm.

To enhance the pumping performance of the IPMC micropump, we designed flap valves to satisfy the requirements of low opening stiffness and high efficiency [20]. The flap valves, which were fabricated from PDMS, a highly flexible material with a low Young's modulus, to ensure the opening stiffness was sufficiently low, were 3 mm long, 2 mm wide, and 0.5 mm thick. We also used photolithography and PDMS molding techniques in the fabrication. When we designed the flap valves, we performed finite element analysis with MSC/NASTRAN^{TM} to determine the optimal configuration.

4. Analyses and experiments

During the development of the IPMC micropump, we performed a series of analyses and experiments not only for design purposes but also for evaluation of the pumping performance of the IPMC micropump. Table 2 summarizes our analyses and experiments.

4.1. Finite element analysis

We used a commercial finite element software, MSC/NASTRAN^{TM}, to analyze the static and vibration characteristics of the IPMC diaphragm with PDMS support and the flap valve. We used 1440 and 840 eight-node solid elements for the IPMC diaphragm and PDMS material, and 845 shell elements for the flap valve. When we performed the static analysis, we used the SOL 106 nonlinear solver. Table 1 lists the material properties of the IPMC diaphragm for the equivalent bimorph beam model. For the vibration analysis, a density of 2500 kg/m^3 was chosen for IPMC diaphragm from the literature [14]. The mechanical properties of the PDMS material with the mixing ratio = 1:10 are as follows: Young's modulus = 750 kPa and density = 920 kg/m^3 [16,17].

For the sake of brevity, we avoided trivial descriptions of the finite element modeling.

4.2. Experimental procedures

To measure the deflection of the fabricated IPMC diaphragm, we used the testing system shown in Fig. 6. The system consists of a digital power supply (Agilent 6811B), a non-contact laser sensor (KEYENCE LK-G80), a computer and a supporting device. The supporting device has two identical PMMA layers with 14 mm diameter openings at the center. The IPMC diaphragm was fixed between the two PMMA layers. To excite the IPMC actuator, we set the power supply to a driving frequency of up to 13 Hz and an applied voltage of up to 3 V.

To measure the pumping characteristics of the IPMC micropump, we used the Agilent 6811B power supply in the experimental setup as shown in Fig. 7. The experimental setup enabled us to measure the flow rate with respect to the driving voltages and the driving frequency at different values of backpressure. Water was used as the running fluid, and we used a voltage range of 1–3 V and a frequency range of 1–11 Hz.

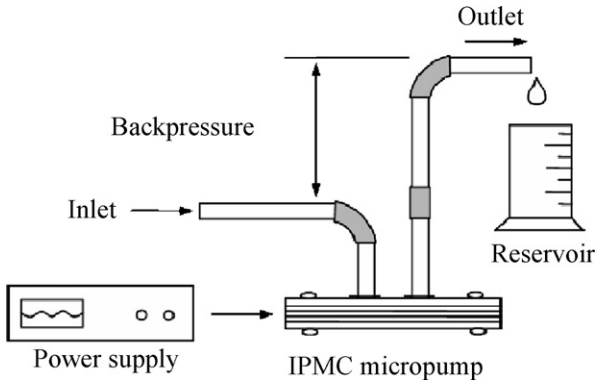

Fig. 7. Experimental setup for testing the flow rate of the micropump.

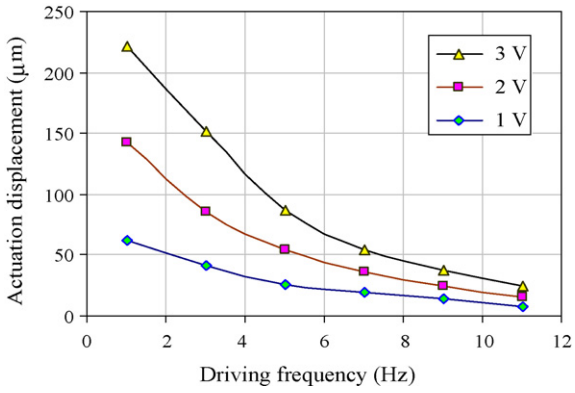

Fig. 8. The actuation displacement vs. driving frequency graph with respect to the various applied voltages.

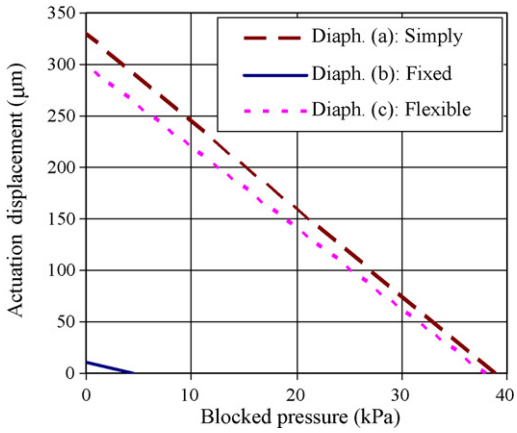

Fig. 10. The actuation displacement vs. blocked pressure graph for the three different support designs.

5. Results and discussion

5.1. Actuation performance of the IPMC diaphragm and verification of the equivalent bimorph beam model

To measure the actuation displacement of the IPMC diaphragm and to verify the equivalent bimorph beam model, we performed an actuation test of the IPMC diaphragm with respect to different levels of applied voltage. Fig. 8 shows the actuation displacement versus the driving frequency graph with respect to different levels of applied voltage. With the same voltage, the actuation displacement reached its highest level at a driving frequency of 1 Hz. We concluded that the IPMC diaphragm shows a good actuation performance at a low driving frequency, possibly because time is needed for the ions inside the IPMC to move to the opposite electrode. On the basis of this explanation, we formulated an equivalent bimorph beam model for a driving frequency of 1 Hz.

Fig. 9 compares the experimental results and the analytical results. The analytical results agree very well with experimental results for the 1 V case and the 2 V case but there is 10% difference for the 3 V case. The error might stem from the fact that the shape of the specimen used to determine the coefficients in Table 1 differed from the shape of our IPMC diaphragm. Even though the maximum relative error between the analysis and the experiment was as high as 10% for the 3 V case, the equivalent bimorph beam model seems capable of predicting the behavior of the IPMC diaphragm for design purposes.

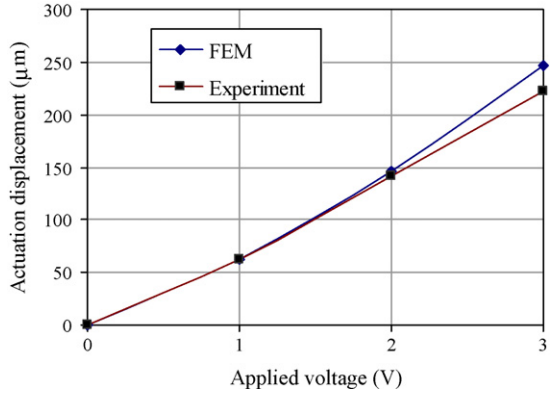

Fig. 9. Verification of the equivalent bimorph beam model: comparison of the numerical and experimental actuation displacement.

5.2. Justification of the concept of flexible support

We claim that a conventional fixed support design constrains the movement of the IPMC diaphragm and that a concept of flexible support can produce a better performance. To justify our claim, we analyzed the actuation displacement versus blocked pressure characteristics of an IPMC diaphragm for the three boundary conditions depicted in Fig. 1. We used the equivalent bimorph beam model for the IPMC actuator. Fig. 10 shows the results for an applied voltage of 3 V.

Under zero blocked pressure, the displacements of the center point of the IPMC diaphragms were found to be 332 μm for diaphragm (a), 9.5 μm for diaphragm (b), and 300 μm for diaphragm (c). Because diaphragm (a) was less constrained than the others, it had the largest actuation displacement of the three cases. The actuation displacement of diaphragm (b), which had a conventional fixed support, is only 3% of the corresponding value for diaphragm (a); and the actuation displacement of diaphragm (c), which had a flexible support, is 90% of the corresponding value for diaphragm (a). Furthermore, the blocked pressure of the IPMC diaphragms was 39 kPa for diaphragm (a), 4.5 kPa for diaphragm (b), and 38 kPa for diaphragm (c). This fact implies that a diaphragm with flexible support can produce a higher output force and a greater actuation displacement than a conventional method with a firmly fixed support.

Table 3
Fundamental frequency of the IPMC diaphragm and the flap valve

Part	Case	Frequency (Hz)
IPMC diaphragm	1 V	64.9
	2 V	75.7
	3 V	81.7
IPMC flap valve		302

5.3. Natural frequencies of the IPMC diaphragm and the flap valve

Given that dynamic properties generally impact on the performance of micropumps, we performed a normal mode analysis to determine the natural frequency of the IPMC diaphragm and the IPMC flap valve. Furthermore, because the IPMC diaphragms were actuated in the first natural mode, we focused solely on the first natural (fundamental) frequencies, which are listed in Table 3. We calculated the natural frequencies for the three applied voltages because the equivalent stiffness of the IPMC actuator differs for each applied voltage in the equivalent bimorph beam model. As shown in Table 3, the fundamental frequencies range from 65 Hz to 82 Hz.

Because a flap valve should have an appropriate natural frequency and opening stiffness to perform well [20], we used finite element analysis to find a better flap valve design. The fundamental frequency of the optimal flap valve was 302 Hz, as listed in Table 3, which is a much higher frequency than the operational frequency of an IPMC actuator (<20 Hz). In addition to the normal mode analysis, we calculated the displacement of the flap valve when pressure was applied to the surface. The displacement was 112 μm under an applied pressure of 500 Pa. With these results, we confirmed that the flap valve had a low level of stiffness and a high natural frequency.

5.4. Pumping performance

With the experimental setup described in Fig. 7, we measured the pumping performance of the IPMC micropump, the results of which are shown in Fig. 11. Fig. 11(a) presents the flow rates of the micropump measured at different voltages and frequencies. As seen in Fig. 11(a), the flow rate initially increases with the driving frequency; it reaches a maximum at 3 Hz, 5 Hz and 3 Hz with applied voltages of 1 V, 2 V, and 3 V, respectively. After the resonance frequency, the flow rate tended to decrease due to the significant decrease of the IPMC diaphragm displacement at high driving frequencies. Note that whereas the fundamental frequencies of the IPMC diaphragm varied from 65 Hz to 82 Hz, as shown in Table 3, and the IPMC diaphragm shows a good actuation performance at lower driving frequency, the resonance frequencies of the IPMC micropump varied from 3 Hz to 5 Hz due to the fluid–structure interaction.

At a working condition of 3 V and 3 Hz, the flow rate reached a maximum value of 760 μl/min, even though the flow rate dropped by half after 10 min due mainly to the electrolysis of the water inside the IPMC. We tried to show how large flow rate the IPMC micropumps could produce, particularly with the assumption that an electrolytically stable inner solvent such as ionic liquids could help increase the durability of the IPMC [21].

Fig. 11(b) shows the flow rate versus the backpressure curve recorded at 3 V and 3 Hz. The micropump exhibits a maximum backpressure of 1.5 kPa. Thus, with the new support structure and the multilayered IPMC actuator, the IPMC micropump produced a higher flow rate and backpressure than the results reported in other works. Note that a backpressure of 0 kPa has no physical meaning in real applications. However, when we design the micropump, the line connecting the zero backpressure point and the zero flow rate point indicates the boundary of operating region. We can therefore choose any point inside the line as an operating point.

During the pumping test, we observed no leakage from the micropump. The good sealing property of the PDMS material solved the sealing problem reported elsewhere [11]. A demonstration of a pumping test is presented at the following URL (available for 1 year after publication): http://konkuk.ac.kr/~nsgoo/ipmcmicropump3V1Hz.mpg.

5.5. Durability results

A durability test for the proposed micropump was performed, and Fig. 12 shows the results for the conditions of 3 V and 1 Hz. The pumping performance decreased rapidly after 5 min, and the flow rate dropped by half after 1 h of operation. The diminishing performance is attributed to the water loss due to electrolysis and to the inherent losses due to natural evaporation; moreover, the surface leakage reduced the performance of the IPMC actuator at operating voltages greater than 1.5 V [9]. Our experiments show that under an applied voltage of 1.5 V our micropump provides

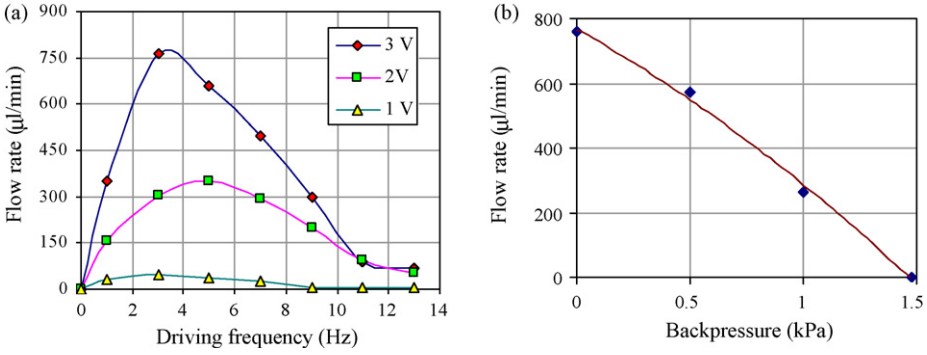

Fig. 11. Pumping performance results: (a) the measured flow rate vs. the driving frequencies at applied voltages of 1 V, 2 V, and 3 V; and (b) the measured flow rate vs. the backpressure at an applied voltage of 3 V and a driving frequency of 3 Hz.

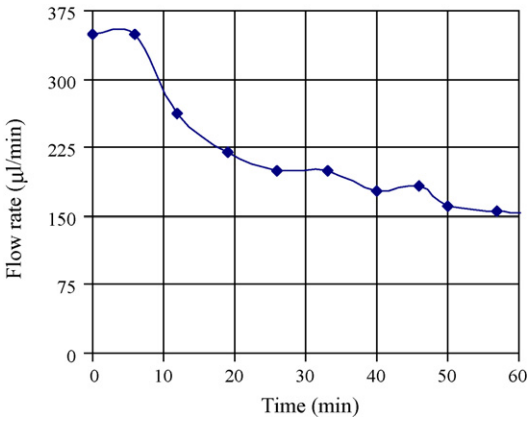

Fig. 12. Flow rate history of the IPMCmicropump at 3 V and 1 Hz.

a consistent output for more than 1 h without any decrease in performance. However, the flow rate became very small: for example, the flow rate was only 50 μl/min at 1 V and 3 Hz as shown in Fig. 11(a).

Our observations showed that the IPMC actuator regained its original pumping performance when no voltage was applied for 15 min. We deduced that the direct contact between the IPMC actuator and the water inside the pump chamber enabled the water to seep into the IPMC actuator, thereby restoring the IPMC actuator and enhancing the durability of the IPMC micropump. However, even though our micropump produces better results than other IPMC micropumps, the durability problem still remains a challenge.

6. Conclusion

We have presented a flap valve IPMC micropump based on the concept of flexible support. A multilayered IPMC was fabricated and characterized for the actuation diaphragm of the micropump. The flap valves were designed and fabricated from PDMS, and the other part of the micropump was fabricated from PMMA with the aid of CNC machining. We performed several experiments along with finite element analysis to investigate the behavior of the IPMC diaphragm and the flap valve, as well as the pumping performance of the IPMC micropump.

We conclude that the flexible support design is an effective concept for the IPMC diaphragm, particularly from the perspective of the actuation displacement versus blocked pressure diagram and the results of the pumping performance. Furthermore, the use of PDMS solves the sealing problem reported elsewhere. The fabricated micropump exhibits a flow rate of 760 μl/min and a backpressure of 1.5 kPa at an applied voltage of 3 V and a resonance driving frequency of 3 Hz, though the pumping performance diminishes rapidly after 5 min due to the electrolysis of water. Even though the proposed IPMC micropump has advantages such as low operational voltage, simple design, no leakage problem and ease of manufacturing, the durability problem remains a challenge if the IPMC micropump is to be used in real applications.

Acknowledgements

This work is supported by Korea Research Foundation Grants (KRF-2006-331-D00085 and KRF-2006-005-J03302). The authors appreciate this financial support.

References

[1] P. Woias, Micropumps-past, progress and future prospects, Sens. Actuators B 105 (2005) 28–38.
[2] N.T. Nguyen, X.Y. Huang, K.C. Toh, MEMS-micropumps: a review, ASME Trans. J. Fluids Eng. 124 (2002) 384–392.
[3] N.T. Nguyen, T.Q. Truong, A fully polymeric micropump with piezoelectric actuator, Sens. Actuators B 97 (2004) 137–143.
[4] T.T. Nguyen, N.S. Goo, Y.S. Yoon, A novel PDMS valveless micropump with a circular lightweight piezo-composite actuator, Key Eng. Mater. 326–328 (2006) 245–248.
[5] W.L. Benard, H. Kahn, A.H. Heuer, M.A. Huff, Thin film shape-memory alloy actuated micropumps, J. Microelectromech. Syst. 7 (2) (1998) 245–251.
[6] S. Boehm, W. Olthuis, P. Bergveld, A plastic micropump constructed with conventional techniques and materials, Sens. Actuator A 77 (1999) 223–228.
[7] O.C. Jeong, S.S. Yang, Fabrication and test of a thermopneumatic micropump with a corrugated P^+ diagram, Sens. Actuators A 83 (2000) 249–255.
[8] R. Zengerle, S. Kluge, M. Richter, A. Richter, A bi-directional silicon micropump, in: Proceedings of the MEMS '95, Amsterdam, The Netherlands, January 29–February 2, 1995, pp. 19–24.
[9] M. Shahinpoor, K.J. Kim, Ionic polymer–metal composites. I. Fundamentals, Smart Mater. Struct. 10 (2001) 819–833.
[10] S. Guo, K. Asaka, Polymer-based new type of micropump for bio-medical application, in: Proceedings of the 2003 IEEE International Conference on Robotic & Automation, Taipei, Taiwan, September, 2003, pp. 1830–1835.
[11] J.J. Pak, J. Kim, S.W. Oh, J.H. Son, S.H. Cho, S.K. Lee, J.Y. Park, B. Kim, Fabrication of ionic-polymer–metal-composite (IPMC) micropump using a commercial Nafion, in: Proceedings of SPIE-Smart Structures and Materials, vol. 5385, 2004, pp. 272–280.
[12] M. Shahinpoor, K.J. Kim, Ionic polymer–metal composites. VI. Industrial and medical applications, Smart Mater. Struct. 14 (2005) 197–214.
[13] S.K. Lee, K.J. Kim, Design of IPMC actuator-driven valve-less micropump and its flow rate estimation at low Reynolds numbers, Smart Mater. Struct. 15 (2006) 1103–1109.
[14] S.K. Lee, H.C. Park, K.J. Kim, Equivalent modeling for ionic polymer–metal composite actuators based on beam theories, Smart Mater. Struct. 14 (2005) 1363–1368.
[15] A. Olsson, G. Stemme, E. Stemme, Diffuser-element design investigation for valve-less pumps, Sens. Actuators A 57 (1996) 137–143.
[16] J.C. Lotters, W. Olthuis, P.H. Veltink, P. Bergveld, The mechanical properties of rubber elastic polymer poly dimethylsiloxane for sensor application, J. Micromech. Microeng. 7 (1997) 145–147.
[17] D. Armani, C. Liu, Re-configurable fluid circuits by PDMS elastomer micromachining, in: 12th International Conference on MEMS, MEMS 99, Orland, FL, USA, 1998, pp. 222–227.
[18] V.K. Nguyen, J.W. Lee, Y.T. Yoo, Characteristics and performance of ionic polymer–metal composite actuators based on Nafion/layered silicate and Nafion/silica nanocomposites, Sens. Actuators B 120 (2007) 529–537.
[19] V.K. Nguyen, Y.T. Yoo, A novel design and fabrication of multilayered ionic polymer–metal composite actuators based on Nafion/layered silicate and Nafion/silica nanocomposites, Sens. Actuators B 123 (2007) 183–190.
[20] K. Junwu, Y. Zhigan, P. Taijiang, C. Guangming, W. Boda, Design and test of a high-performance piezoelectric micropump for drug delivery, Sens. Actuators A 121 (2005) 156–161.
[21] M.D. Bennett, D.J. Leo, Ionic liquids as stable solvents for ionic polymer transducers, Sens. Actuators A 115 (2004) 79–90.

Biographies

Thanh Tung Nguyen received the BE degree in aerospace engineering from the Vietnam-France Program for Excellence (PFIEV), Ho Chi Minh City University of Technology, Vietnam, and the MSc degree in aerospace engineering from Konkuk University, Korea, in 2004 and 2007, respectively. He is currently a PhD student with the Department of Mechanical Engineering and a research assistant with the Opto-Mechanics Research Lab at the State University of New York at Binghamton. His research interests are micropumps, MEMS, and electronics packaging.

Nam Seo Goo graduated from Department of Aeronautics Engineering of Seoul National University with honors in 1990, and got master and PhD degrees in Department of Aerospace Engineering at the same university in 1992 and 1996, respectively. His PhD degree was on the structural dynamics of aerospace systems. As soon as he got a PhD degree, he entered the agency for defense development as a senior researcher. After four years' service, he moved to Kyungpook National University as a research associate. He joined Department of Aerospace Engineering in Seoul, Korea in 2002, currently serving an associate professor of Department of Advanced Technology Fusion. He has more than 100 technical publications. He was nominated as a Young Scientist by Korea Science & Engineering Foundation, in 2003 and included in Marqui's Who's who in the World. His current research interests are structural dynamics of small systems, smart structure and material, and MEMS applications.

Vinh Khanh Nguyen received his PhD in chemical engineering (polymers) for his work on the polypropylene ionomer nanocomposite at Chonbuk National University, Korea in 2005. He then joined and worked as a research fellow at the Artificial Muscle Research Center of Konkuk University, Korea. In 2007, he joined the Faculty of Chemical Engineering at Hochiminh City University of Technology, Vietnam. His research interests include the tailoring and design of polymer nanocomposites, ionomers, electroactive polymers and MEMS.

Youngtai Yoo graduated from the Virginia Polytechnic Institute and State University in 1988, and received his PhD in chemical engineering. He worked at Eastman Kodak Company as a research scientist until 1991. Then he joined the Department of Materials Chemistry and Science at KonKuk University. His research interests include biomedical polymers, fuel cells and actuators.

Seungbae Park received his PhD at Purdue University in 1994. Dr. Park began his professional career at IBM Microelectronics Division as a development and the reliability engineer responsible for the assurance of IBM's flip chip technology in both leaded and lead-free solders and high performance packaging. After 7 years at IBM, Dr. Park started his academic career at the State University of New York at Binghamton in 2002. He is an associate professor and has more than 70 technical publications and many US patents. Dr. Park has been chairing iNEMI's Modeling and Simulation Technical Work Group, "Electronics Packaging" council in the Society of Experimental Mechanics. He is "Electronics and Photonics Packaging" division representative of IMECE 2007 and the chair of Electronics Packaging division of Society of Experimental Mechanics. Dr. Park's research interest is physical reliability for microelectronics and MEMS packaging.